

Mars 2020 Entry, Descent and Landing Instrumentation 2 (MEDLI2)

Helen H. Hwang,¹ Deepak Bose,² and Todd R. White³
NASA Ames Research Center, Moffett Field, CA 94035, USA

Henry S. Wright,⁴ Mark Schoenenberger,⁵ Christopher A. Kuhl,⁶ and Dominic Trombetta⁷
NASA Langley Research Center, Hampton, VA 23681, USA

Jose A. Santos⁸
Sierra Lobo, Inc., Moffett Field, CA 94035, USA

Tomo Oishi⁹
Jacobs Technology, Inc., Moffett Field, CA 94035, USA

Christopher D. Karlgaard¹⁰
Analytical Mechanics Associates, Inc., Hampton, VA 23681, USA

Milad Mahzari¹¹
Analytical Mechanics Associates, Inc., Moffett Field, CA 94035, USA

Steven P. Pennington¹²
Science Systems and Applications, Inc., Hampton, VA 23681, USA

Abstract

The Mars Entry Descent and Landing Instrumentation 2 (MEDLI2) sensor suite will measure aerodynamic, aerothermodynamic, and TPS performance during the atmospheric entry, descent, and landing phases of the Mars 2020 mission. The key objectives are to reduce design margin and prediction uncertainties for the aerothermal environments and aerodynamic database. For MEDLI2, the sensors are installed on both the heatshield and backshell, and include 7 pressure transducers, 17 thermal plugs, and 3 heat flux sensors (including a radiometer). These sensors will expand the set of measurements collected by the highly successful MEDLI suite, collecting supersonic pressure measurements on the forebody, a pressure measurement on the aftbody, direct heat flux measurements on the aftbody, a radiative heating measurement on the aftbody, and multiple near-surface thermal measurements on the thermal protection system (TPS) materials on both the forebody and aftbody. To meet the science objectives, supersonic pressure transducers and heat flux sensors are currently being developed and their qualification and calibration plans are presented. Finally, the reconstruction targets for data accuracy are presented, along with the planned methodologies for achieving the targets.

¹ Aerospace Engineer, Email: helen.hwang@nasa.gov

² Former Aerospace Engineer, AIAA Associate Fellow

³ Aerospace Engineer, AIAA Senior Member

⁴ Aerospace Engineer

⁵ Aerospace Engineer, AIAA Senior Member

⁶ Aerospace Engineer

⁷ Aerospace Engineer

⁸ Mechanical Engineer

⁹ Engineering Specialist

¹⁰ Supervising Engineer, AIAA Senior Member

¹¹ Senior Systems Engineer

¹² Senior Engineer/Scientist

I. Introduction

This paper introduces the Mars Entry Descent and Landing Instrumentation 2 (MEDLI2) concept for NASA's Mars 2020 mission. Mars 2020 is a flagship-class mission, scheduled for launch in 2020, with science and technology objectives to help answer questions about habitability of Mars as well as to demonstrate technologies for future human expedition. MEDLI2 is a suite of instruments located on the heatshield and backshell of the Mars 2020 entry vehicle. Some of the sensors are embedded in the thermal protection system (TPS) materials, and others are mounted on the inner mold line of the aeroshell. The objectives of MEDLI2 are to gather critical aerodynamics, aerothermodynamics and TPS performance data during the Entry, Descent and Landing (EDL) phase of the mission. MEDLI2 builds from the success of the MEDLI instrumentation [1] flown on the Mars Science Laboratory (MSL) mission in 2012. The MEDLI instrumentation suite measured surface pressure and TPS temperature on the heatshield during MSL entry into Mars. MEDLI data has since been used for reconstruction of aerodynamic drag, vehicle attitude, *in situ* atmospheric density, aerothermal heating, transition to turbulence, in-depth TPS performance and TPS ablation. [2,3] In addition to validating predictive models, MEDLI data has highlighted extra margin available in the MSL forebody TPS. Because the Mars 2020 entry vehicle is nearly identical to that flown for MSL, the additional mass found on the forebody TPS could potentially be removed if needed.

MEDLI2 expands the scope of instrumentation, adding sensors on the backshell and focusing on quantities of interest not addressed in the MEDLI suite. Additional sensor types are included with the layout on the TPS customized to meet the enhanced objectives. This paper provides the key motivation and governing requirements that drive the choice and the implementation of MEDLI2's sensor suite. The implementation considerations of sensor selection, qualification, and calibration are described. The challenges associated with sensor development for pressure transducers and heat flux sensors are also described.

II. Goals and Objectives

NASA's exploration and technology roadmaps call for capability advancements in Mars EDL systems to enable increased landed mass, a higher landing precision, and wider planetary access. [4] It is also recognized that these ambitious EDL performance goals must be met while maintaining a low mission risk to pave the way for future human missions. As NASA is engaged in developing components of future EDL systems and technologies via testing at Earth, flight instrumentation such as MEDLI and MEDLI2 on existing Mars missions is providing valuable engineering data for performance improvement, risk reduction, and an improved definition of entry loads and environment.

MEDLI2 has the following goals:

- 1) Acquire flight data to define the entry aerothermal environments and reduce aerothermal uncertainties
- 2) Acquire flight data to reduce entry vehicle TPS mass
- 3) Acquire flight data to improve future aerocapture and EDL performance

The abovementioned goals for MEDLI2 will be met via reconstruction of aerothermal environment, aerodynamic performance, and TPS in-depth performance from the sensor data. Specific objectives for each discipline have been developed for maximum impact on the goals. These objectives drive the top level instrument requirements to be described later in the paper. For aerothermal and TPS goals, the objectives are defined such that they reduce design margins and prediction uncertainty. For aerodynamics goals, the objectives are defined similarly to reduce uncertainty and enable validation of the aerodynamic database.

III. Science Requirements

A set of top-level science requirements are defined to set reconstruction and measurement targets for MEDLI2. The requirements are then distilled further to ensure that sensor accuracy, measurement range, and data sampling rate are adequate to meet MEDLI2 objectives. A concise list of science requirements is as follows:

Aerothermodynamics and TPS:

- 1) Reconstruct forebody aeroheating
- 2) Determine forebody TPS temperatures
- 3) Reconstruct aftbody aeroheating
- 4) Measure aftbody heat flux

Aerodynamics:

- 1) Reconstruct hypersonic and supersonic aerodynamic axial force coefficient
- 2) Reconstruct wind relative vehicle attitude

- 3) Reconstruct atmospheric density and winds
- 4) Reconstruct vehicle Mach number

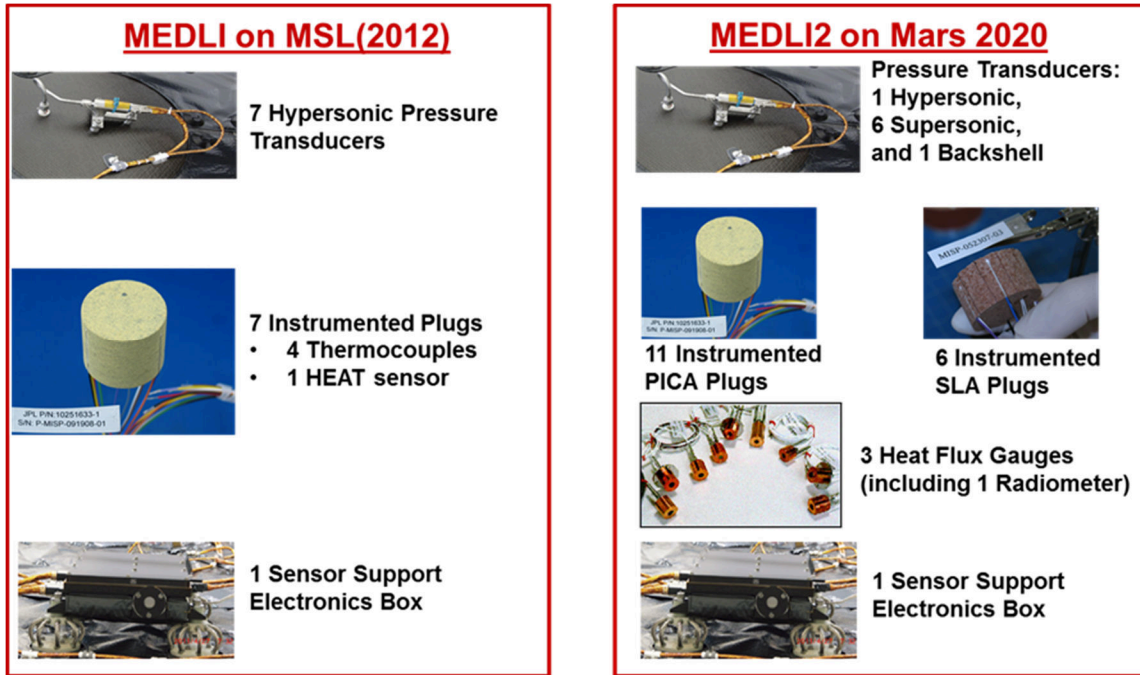


Figure 1. MEDLI and MEDLI2 instrument suites.

IV. Sensors and Development Challenges

Figure 1 shows the instruments included in MEDLI2 suite. The MEDLI instrumentation suite is also shown for comparison. Similar to MEDLI, pressure transducers and thermocouples form a bulk of the instrumentation. MEDLI2 has additional sensor types such as heat flux sensors, instrumented SLA-561V backshell plugs, and pressure transducers for supersonic flight and backshell measurements.

A. Pressure Transducers

In order to meet the science objectives, three types of pressure transducers have been selected. Each type of transducer will be calibrated for a specific measurement range and required accuracy. The hypersonic stagnation pressure will be measured using a MEDLI flight spare pressure transducer for the 0–35,000 Pa range that spans the entire test period including the peak dynamic pressure environment. One of the key findings from MEDLI was that the hypersonic pressure transducers do not provide sufficient accuracy at lower pressures during supersonic flight. Therefore, a separate set of supersonic transducers are included that are accurate over the 0–7000 Pa range. A third type of pressure transducer has been selected to measure low pressures of 0–700 Pa expected on the backshell of the vehicle. The layout of the sensors on the heatshield and backshell are shown in Fig. 2. The locations of the pressure transducers on the forebody are defined using an optimization algorithm [5] that minimizes errors in reconstruction of vehicle angle of attack and side-slip.

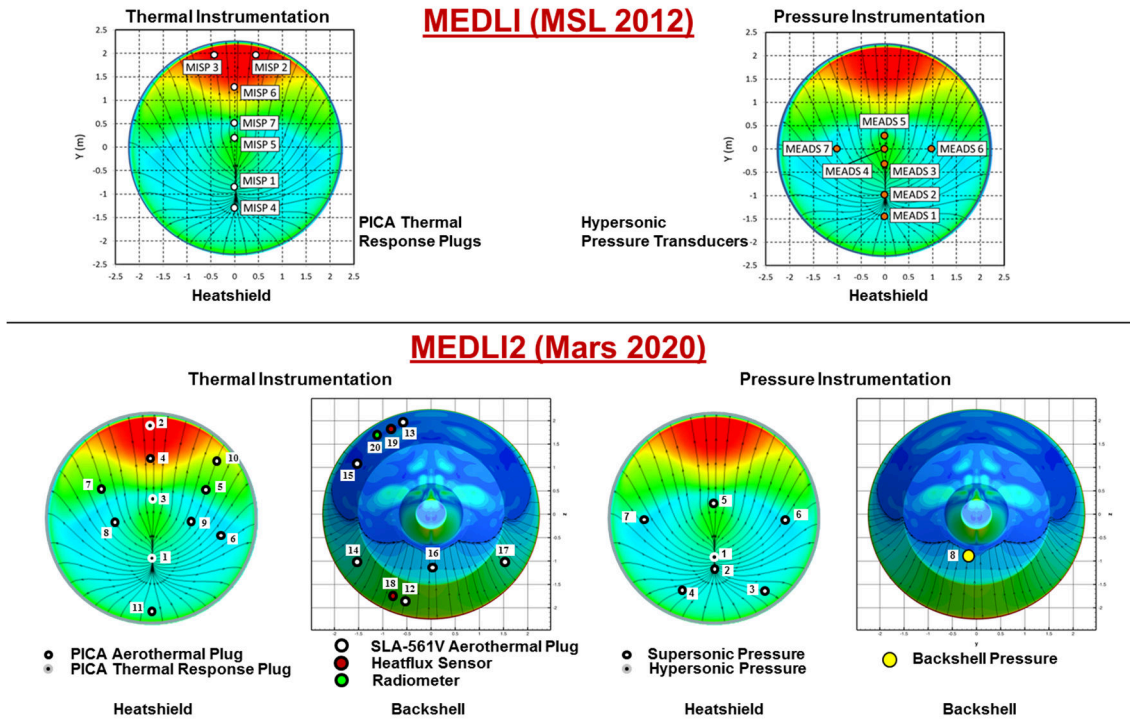


Figure 2. Sensor locations for MEDLI and MEDLI2.

A total of 6 supersonic sensors on the heatshield will be used to reconstruct vehicle drag coefficient, attitude, and *in situ* atmosphere in flight until parachute deployment. The main challenge for implementing the supersonic sensors is that no commercially available pressure sensor exists that can meet the required pressure range and survive the extreme temperature environments in space ($-130\text{ }^{\circ}\text{C}$). Several options were evaluated, including the use of survival heaters or modifying existing pressure sensor designs. Ultimately it was decided to modify an existing pressure sensor using a state-of-the-art piezoresistive sensing unit. The advantages of this approach are that the sensors will have larger output signal, a more accurate measurement range, and can withstand the predicted low thermal environments. Tethering the active electronics of the sensors and relocating them to the Sensor Support Electronics (SSE) data acquisition system eliminates the low temperature survival concerns. Some of the challenges with this approach are that the gauges are more susceptible to damage during installation (bonding and wiring) and require significant thermal characterization during sensor calibration.

A proof-of-concept sensor was demonstrated by disassembling a commercially available pressure sensor and replacing the foil-backed strain gauge with a semiconductor piezoresistive gauge. A 12-point calibration of the sensor was then performed in tandem with an unmodified pressure sensor. Testing showed that the effective output signal (gauge factor) was increased by more than 60 times (46 mV compared to 0.75 mV). Plans are underway for the detailed design, build, and testing of the modified supersonic pressure sensors, with extensive testing and calibration scheduled for the fall of 2016.

One aftbody base pressure sensor will be used to reduce uncertainty in drag coefficient reconstruction. It is anticipated that the temperatures on the aftbody will be no colder than $-55\text{ }^{\circ}\text{C}$, due to the aftbody facing the sun during most of interplanetary cruise phase, hence a commercially available pressure sensor with active electronics will be used.

B. Thermocouples

Thermocouples (TCs) will be embedded in the TPS using instrumented plugs as shown in Fig. 1. Unlike MEDLI, MEDLI2 TCs will focus on near surface temperatures. Two types of TCs will be used. Type R TCs will be used at shallower depths ($< 0.1\text{ in}$) and Type K will be used at greater ($\geq 0.1\text{ in}$) depths. In order to capture the turbulent footprint and transition phenomena, an increased number of TC plugs are distributed over the heatshield as shown in Fig. 2. Two types of plugs are chosen. The Aerothermal plugs consisting of one near-surface TC will map the aerothermal environment on the forebody and backshell. The Thermal Response plugs will contain three TCs and

measure in-depth response of the TPS material. All forebody plugs will be made from Phenolic Impregnated Carbon Ablator (PICA), which is the forebody TPS. The aftbody plugs will contain one Type K TC each and will be made from the backshell TPS, SLA-561V. The aftbody plugs will map the aerothermal environment in the attached and separated flow regions of the backshell, and also span both conical surfaces.

C. Heat Flux Sensors and Radiometer

The lower levels of heating ($< 25 \text{ W/cm}^2$) predicted on the backshell creates options for more accurate sensors for direct measurement of heat flux, and a separate measurement of radiative heating. Candidate locations for these sensors are shown in Fig. 2. These locations allow measurements of the convective and radiative environments on the leeside separated flow region, as well as the convective environment on the windside attached flow region.

MEDLI2 has tested candidate commercially available heat flux gauges for accuracy and survivability. The sensors included Gardon gauges, a thermopile, and Schmidt-Boelter gauges. Benchtop tests were performed and the sensors were evaluated for time response, measurement accuracy, signal-to-noise ratio, and survivability for a given maximum expected heat load. Two of the six sensor candidates subsequently underwent further testing to verify functionality after exposure to environmental and aerothermal loads. The environmental tests consisted of random vibration testing at $18.4 \text{ g}_{\text{rms}}$, shock testing up to $4,000 \text{ g}$, and thermal vacuum cycling between $+70 \text{ }^\circ\text{C}$ and $-85 \text{ }^\circ\text{C}$. An arcjet test at the NASA Ames Panel Test Facility (PTF) was conducted after completion of all the environmental tests to study sensor response upon exposure to a convective heat flux. Test results verified functionality after the environmental and arcjet tests; quantitative analysis of the arcjet test data is currently underway. Several challenges exist in interpreting the data, as the arcjet calibration comparisons are conducted using a water-cooled copper plate, while the candidate sensors were tested in panels of TPS material. The difference between the “cold wall” heat flux on the calibration plate compared to the “hot wall” heat flux on the TPS panel must be considered in comparing the measured values for both tests. In addition, post arcjet test inspection revealed a coating on the surface of each sensor, most likely a by-product of the TPS decomposition and ablation process. The surface coating’s effect on the measurements is currently an area of study. A Schmidt-Boelter gauge was ultimately selected based on its performance during benchtop testing.

In addition to the thermal plugs and heat flux measurements described above, MEDLI2 will also include a radiometer to make a direct measurement of radiative heating. The radiometer is a specialized version of the selected heat flux sensor that uses a sapphire window to block convective heat flux from the thermopile sensing element while still allowing the radiant heat flux to be detected. MEDLI2 identified several of the important performance parameters for the aftbody radiometer, based on predictions from state-of-the-art flow field radiation modeling tools. [6] Because radiative heating is a significant fraction of the overall heating on the aftbody, the radiometer will have a measurement range comparable to that of the heat flux sensor ($0\text{--}15 \text{ W/cm}^2$). It will also have an identical electrical output and wiring connections as the heat flux sensors.

Additionally, the radiometer will have a body-style identical to that of the heat flux sensor, to minimize the number of installation procedures and qualification tests. Both the heat flux and radiometer sensors will be passively cooled. Figure 3 below shows the body style for both the heat flux sensor and radiometer, which includes a large cylindrical heatsink. The sensor will attach via three fasteners through a copper heatsink; the heatsink resides inside the aftbody structure, and the sensing element is installed flush with the outer mold line of the surrounding TPS.

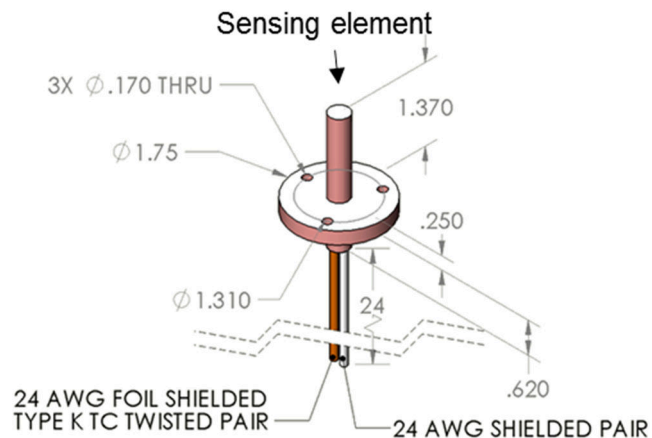


Figure 3. Heatflux Sensor / Radiometer body style. Dimensions are in inches.

Aeroheating predictions for the Mars 2020 entry indicate the entire aftbody will experience measurable radiative heating. The radiometer will be located in the region of highest predicted radiative heating, in both magnitude and integrated load, on the leeward shoulder near the vehicle centerline.

Two important design considerations for the MEDLI2 radiometer are view factor to the sensing element, and the optical properties of the radiometer window. The MEDLI2 radiometer will have a wide view angle ($\sim 150^\circ$) compared to that the narrow view angle (9°) of the recessed radiometer flown on the Apollo 4 heatshield. [8] A wide view angle combined with the predicted highly-radiating aftbody flow-field are expected to lead to a substantial signal. Figure 4 shows the projection of radiance versus view angle, where the center point is normal to the radiometer and polar angle is increasing away from the center. The radiometer will observe all radiance contained within the dashed line.

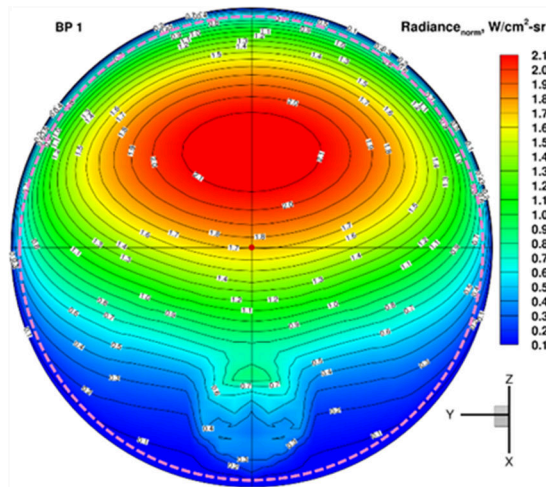


Figure 4. Surface projected radiance at time of peak radiative heating and radiometer view factor [6].

The optical properties of the sapphire radiometer window will be evaluated to characterize how much of the radiative heating will be transmitted into the sensing element. Figure 5 below shows VUV and IR band systems measured experimentally at MSL and Mars 2020-relevant conditions. The sapphire window is not expected to significantly attenuate the incident radiance, as sapphire windows typically have a flat spectral transmittance range below 5000 nm. A remaining question is how deposition of the ablation products may alter the optical properties on the window during entry. One potential method to characterize this effect could be to calibrate a radiometer to a radiant heat source, test the radiometer embedded in a TPS panel in simulated entry convective environments in an arcjet, then repeat the calibration with the same radiant source. Changes in readings during the second calibration could indicate the extent of the effect of ablation products.

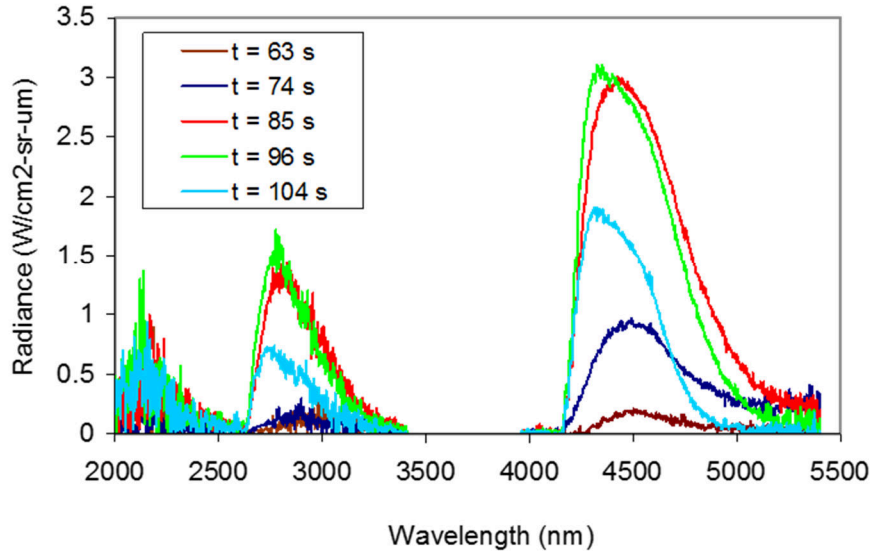


Figure 5. IR spectra as measured in shock tube facility. Times are for the MSL reconstructed trajectory [7].

V. Sensor Testing: Qualification and Calibration

Together, the pressure, temperature, heat flux, and radiation heating sensors form a new suite of instrumentation for Mars entry vehicles. All of the sensors will be tested in a qualification program to ensure flight readiness. The qualification will include thermal and mechanical survivability under flight-relevant aerothermal, shock, vibration, and thermal vacuum conditions. In addition, the sensors will be calibrated prior to installation.

A. Pressure Sensor Testing

Calibration of the pressure measurement system will be conducted to compute pressure as a function of voltage, and sensor and electronics temperature. The calibration approach will leverage the methodology utilized for MEDLI [9], which was based on an industry standard approach that was also successfully implemented for the Shuttle Entry Atmospheric Data System (SEADS) [10] and the Aeroassist Flight Experiment (AFE) [11].

The calibration approach acquires a set of input pressure data vs. transducer output voltage at various temperatures to define a transducer sensitivity (scale factor), non-linearity, and bias (zero offset) as a function of pressure head and electronics temperatures. The coefficients are collected by a process that uses an increasing/decreasing application of pressure over the operating range of the transducer. The number of pressure set points can vary depending on project requirements. A total of 13 pressure points were utilized for MEDLI calibration. A series of pressure versus voltage output data sets are obtained at applicable operating temperatures to define the thermal sensitivity of the pressure sensitivity and zero offset. The number of temperature set points can also vary. A total of 14 temperature set points were used for MEDLI calibration.

The calibration method makes use of a model of the form $p = a_0(T_1, T_2) + a_1(T_1, T_2)V + a_2(T_1, T_2)V^2$, where T_1 is the pressure transducer temperature, T_2 is the SSE temperature, V is the Voltage, and p is the pressure. The coefficients a_0 , a_1 , and a_2 are the bias, sensitivity, and non-linearity, respectively. These coefficients are determined from a least-squares fit of pressure vs. voltage data at specific temperature setpoints. By varying the temperature setpoints, a database of calibration coefficients can be constructed for an empirical model. The model uses spline interpolation to determine the coefficients as functions of the two temperatures.

As described by Karlgaard et al. [12], reconstruction of the MSL entry with the onboard inertial measurement unit and MEDLI flight data found that the pressure transducers likely experienced a small hysteresis in their response as they went through the peak pressure pulse of entry and decelerated through the supersonic regime leading to parachute deploy. Preflight calibration data showed that this hysteresis was present to varying degrees for each transducer. The effects were within the uncertainty requirements and in general could not be characterized or modeled with the available data. It is likely that the two lateral pressure ports on MSL saw different hysteresis responses during entry

which resulted in an indicated (erroneous) sideslip which increased as the vehicle decelerated to low supersonic speeds. This phenomenon will be factored in the selection process of the MEDLI2 pressure transducers and calibration procedures will attempt to replicate the time history of the expected Mars 2020 entry pressure pulse to better characterize the hysteresis response of the flight transducers. The project will either reduce the hysteresis response or develop a model to characterize each transducer.

B. Thermal Plug Testing

As with the pressure sensors, the thermal plugs for both the heatshield and backshell will undergo a qualification test program involving random vibration, shock and thermal vacuum testing to demonstrate compliance with mechanical loads and thermal environments for the Mars 2020 mission. Upon completion of the environmental testing, the same test articles will then be subjected to arcjet testing to represent appropriate flight-like aerothermal environments. Both the heatshield PICA and the backshell SLA-561V instrumented plugs will undergo flight lot acceptance testing prior to flight hardware delivery.

No formal calibration activity is required for the completed instrumented plug assembly. The thermocouples embedded within the plug, however, are procured as Special Limits of Error wire, which comply with known uncertainties traceable to ASTM E230 and the ITS-90 tables and are more accurate than thermocouples with standard tolerances.

C. Heat Flux Sensor and Radiometer Testing

Both the radiometer and heat flux sensor will be calibrated using a radiant heat source, including an infrared (IR) lamp with a NIST traceable reference gauge. The reference gauge is a water-cooled Gardon gauge specified by the manufacturer's calibration and absorptivity of its coating. By comparing the measurements of the heat flux sensor (and the radiometer) to the reference gauge, a custom calibration can be performed. For the radiometer, the transmissivity of its window is expected to attenuate wavelengths above 5000 nm. During calibration, this effect will be measured. The heat flux sensors will be qualified for flight through a combination of testing and analysis, similar to the qualification approach for the thermal plugs.

VI. System Architecture and Operation

MEDLI2 sensor data will be collected by the SSE, which is powered by a 28 V_{DC} source from the Mars 2020 avionics. The SSE contains three internal boards: an analog board, a shield board, and a digital board. The SSE chassis is mounted on the inside of the heatshield just below the Rover's Multi-Mission Radioisotope Thermoelectric Generator, which aids in keeping the SSE electronics at a relatively benign temperature of 20 °C to 30 °C. The SSE performs the following supporting functions: power conditioning, sensor excitation, cold junction compensation for the thermocouple measurements, sampling, multiplexing, signal conditioning, analog-to-digital conversion, packetization, and data communication with the Mars 2020 Descent Stage Power and Analog Module. The SSE will sample all measurements at 16 samples per second (sps), but the data will be decimated and packetized to provide data rates of 1, 4, 8, and 16 sps depending on the sensor type.

A significant change for MEDLI2 is the oversampling of the pressure measurements by the SSE. To accomplish this, a 16:1 main multiplexer feeds a 2-pole filter into a separate 14-bit A/D located on the digital board. All pressure measurements will be sampled and averaged at 256 times every 1/8 of second. This average is then packetized into a single word; this process is repeated 8 times per 1-second frame. Oversampling reduces the noise floor, thus improving the signal-to-noise ratio while also reducing the vibration sensitivity.

Harnessing for power, data communication, sensor excitation, and signal return will form a network throughout the vehicle, including both the heatshield and backshell. The associated cables will be passed through a 5/8 inch cable cutter at the backshell-to-heatshield separation interface.

MEDLI2 will be activated about five hours prior to atmospheric entry interface to aid in establishing thermal equilibrium of the electronic components, and will begin collecting data 10 minutes prior to entry. The MEDLI2 instrumentation system will continue collecting data during the critical test period of hypersonic and supersonic portions of the trajectory and will be powered off shortly before the heatshield is jettisoned, after parachute deployment and eventual deceleration to subsonic speeds. The complete MEDLI2 data set will be telemetered back to earth after surface landing and health status checks have occurred.

VII. Reconstruction Targets

MEDLI2 science objectives rely on successful reconstruction of aerodynamic, aerothermal, and TPS performance using sensor data and physics based modeling. The physics based models are often necessary to bridge the gap between

sensor measurements and quantities of interest. Table 1 presents the quantities of interest and targeted reconstruction accuracy.

Table 1. MEDLI2 Reconstruction Targets

Quantity of Interest	Reconstruction Target	Relevant Sensors
Forebody Reconstructed Heating	$\pm 15 \text{ W/cm}^2$	Forebody Thermocouples
Boundary Layer Transition	$\pm 1 \text{ second}$	Forebody Thermocouples
In-depth Temperatures	$\pm 50 \text{ }^\circ\text{C}$	Forebody Thermocouples
Aftbody Reconstructed Heating	$\pm 3 \text{ W/cm}^2$	Aftbody Thermocouples
Aftbody Heat Flux	$\pm 1 \text{ W/cm}^2$	Heat Flux Sensor/Radiometer
Axial Force Coefficient	$\pm 2\%$	All Pressure Transducers
Vehicle Attitude	$\pm 0.5 \text{ degrees}$	Supersonic Pressure Transducers
Atmospheric Winds	$\pm 10 \text{ m/s}$	Supersonic Pressure Transducers
Atmospheric Density	$\pm 5\%$	Forebody Pressure Transducers
Mach Number	± 0.1	Forebody Pressure Transducers
Aftbody Pressure	$\pm 4 \text{ Pa}$	Aftbody Pressure Transducer

A. Pressure Measurements

A linear covariance analysis of the pressure data processing algorithm was conducted to derive pressure measurement accuracies. The requirement for the base pressure measurement accuracy is 4 Pa. This requirement is based on the resolution required to reconcile the reconstructed axial force coefficient with the base pressure correction. No analysis tools are required to transform the aftbody pressure measurement, unlike the forebody measurements which utilize an algorithm to transform measured pressures into the science data products (angle of attack, density, winds, etc.).

The results from the linear covariance analysis method indicate that 1% of reading errors are acceptable for meeting the science requirements. One exception is the angle of attack requirement, which will be investigated further to determine if certain modeling assumptions are overly conservative or if additional algorithmic enhancements can improve the reconstruction performance.

Table 2. Pressure Measurement Accuracies

Measurement	Accuracy (3σ)	Measurement Range
Hypersonic Pressure	1% of reading	1650–35,000 Pa
Supersonic Pressure	1% of reading	650–7,000 Pa
Backshell Pressure	4 Pa	40–700 Pa

Table 2 summarizes the pressure measurement accuracies and ranges that are required in order to meet the reconstruction targets in Table 1. Note the low range for the hypersonic measurement (1650 Pa) corresponds to the pressure measured behind the bow shock at a freestream dynamic pressure of 850 Pa. The supersonic low pressure range corresponds to the pressure measurement behind the bow shock at the 3σ low dynamic pressure at parachute deployment of 400 Pa (pending update from trajectory team).

The pressure sensor basic processing algorithm combines pressure measurements with navigation filter outputs to produce estimates of the science data products. The algorithm is an enhanced version of that used for MEDLI reconstruction [12], and the mathematical details can be found in [5]. At a high level, the algorithm can be described as a weighted least-squares method in which best-fit estimates of the atmospheric conditions (pressure, density, and winds) are computed, given the inertial state of the vehicle (position, velocity, and attitude) and a model of the surface pressure distribution. High fidelity atmospheric model data can be incorporated in the form of a table lookup vs. altitude, as an initial guess of the atmospheric profile. Low-fidelity models can also be utilized to propagate the atmospheric state forward in time between pressure measurement samples in order to better initialize the iteration performed at each sample. A flowchart of the process is shown in Fig. 6.

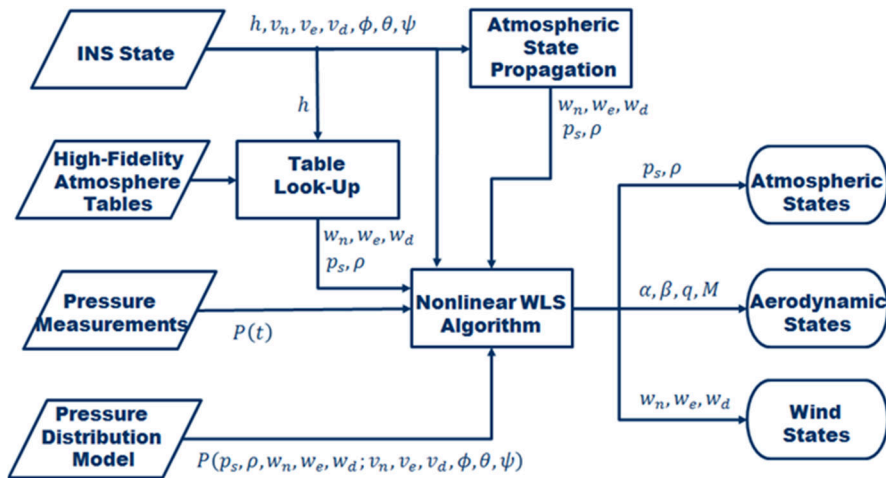


Figure 6. MEDLI2 Data Processing Algorithm.

A linear covariance analysis tool based on the MEDLI2 data processing algorithm has been created for mapping input uncertainties through the nonlinear algorithm to the output uncertainties. By specifying pressure measurement errors, uncertainties in the corresponding science data products can be generated. Results of the linear covariance analysis tool applied to the current MEDLI2 system design specifications are shown in the following figures. Figure 7 shows the science requirements compliance for dynamic pressure (as a proxy for axial force coefficient) and density in the hypersonic flight regime. The results indicate that the system meets the requirements in this flight regime.

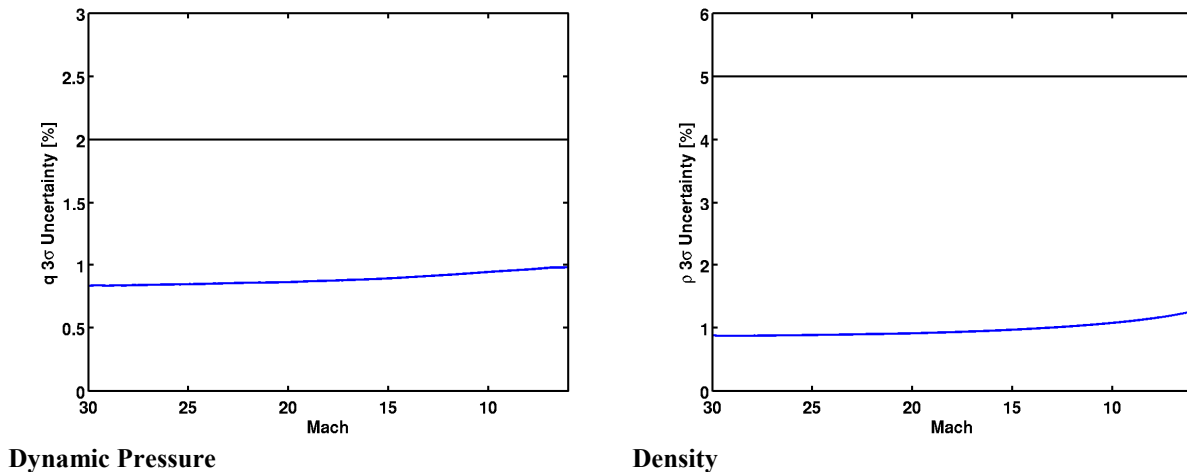


Figure 7. Science Requirements Compliance in Hypersonic Regime.

Figure 8 shows the science requirements for aerodynamic flow angles, dynamic pressure, density, Mach number, and winds in the supersonic flight regime. These results indicate that the requirements are met with the exception of the aerodynamic flow angles at Mach 2.4. This point corresponds to the time of the Entry Ballast Mass (EBM) jettison event, which changes the trim angle from approximately -20 degrees to zero, in preparation for parachute deployment which occurs near Mach 2.0. The reason for this degradation is that the port layout was optimized for pre-EBM trim angle. The impact of this loss of science in the post-EBM flight regime is currently under investigation.

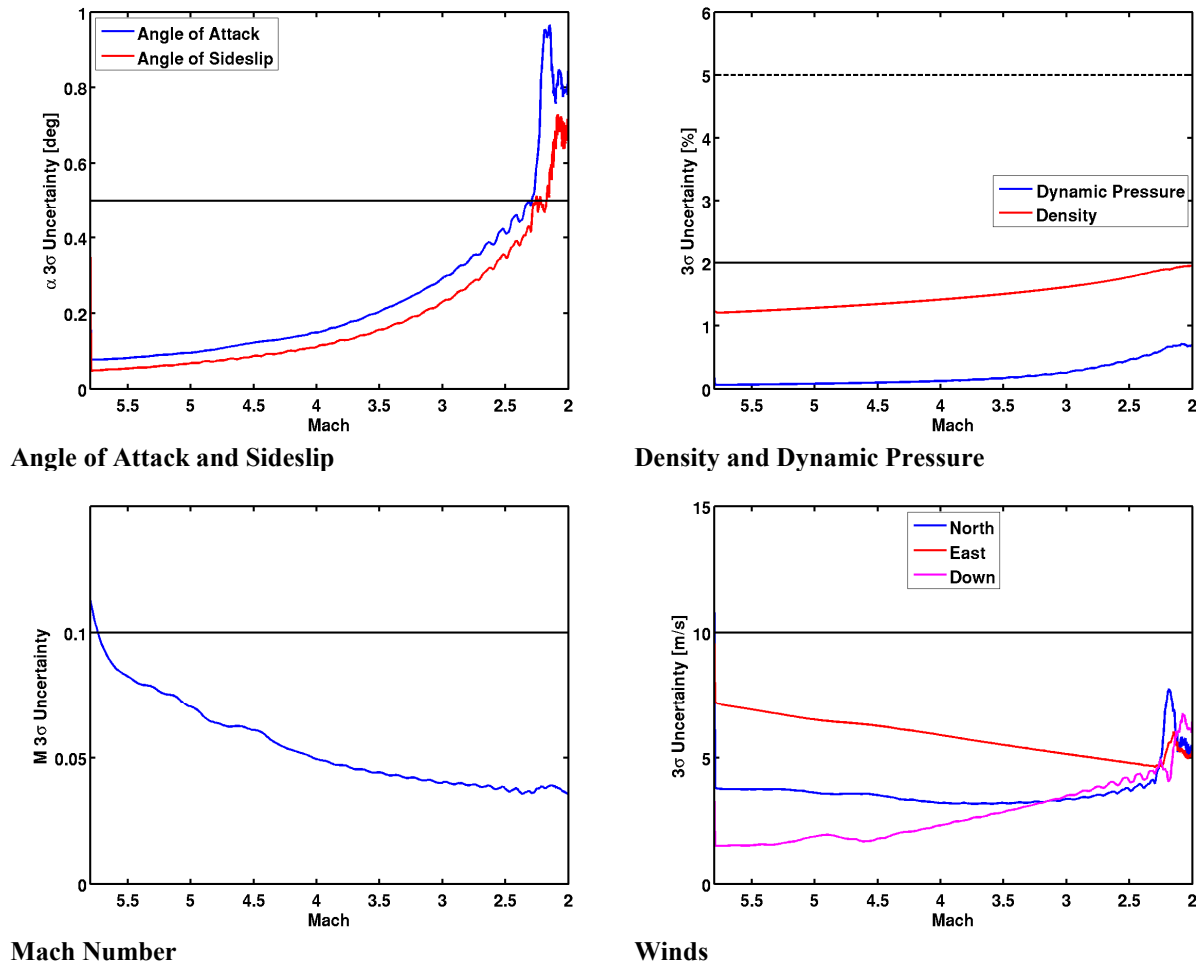


Figure 8. Science Requirements Compliance in Supersonic Regime.

B. Thermal Measurements

MEDLI utilized inverse techniques with in-depth thermocouple data to reconstruct MSL’s surface heating at the thermal plug locations. References 7 and 13 describe the data analysis methodology, techniques, and results related to that study. Surface heating was estimated using a whole-time domain least squares technique which minimizes the sum of squared differences between thermocouple data and temperature predictions by TPS response code FIAT. Tikhonov regularization technique was utilized to alleviate oscillations that occur in such function estimation problems. The original plan for thermal measurement reconstruction was to estimate surface film coefficient as a function of time while keeping other surface parameters fixed at their computational fluid dynamics (CFD)-predicted or FIAT-calculated values. The advantage of this approach is that the reconstructed surface film coefficient can be readily compared with CFD predictions to evaluate the accuracy of computational models in predicting surface heating. However, this approach did not work as planned due to inaccuracies of PICA equilibrium gas–surface chemistry model. The model is known to over-predict recession and wall enthalpy at MSL’s low heating conditions. Inaccurate prediction of wall enthalpy limits the ability to reconstruct the film coefficient.

No validated finite-rate models exist for PICA gas-surface chemistry in the Martian atmosphere. Consequently, the observed lack of substantial recession in flight and the known over-prediction by FIAT equilibrium chemistry models motivated the application of another bounding approach where surface heating was estimated without recession. The absence of surface chemistry calculations in reconstruction meant that the surface heating profile estimated using this approach included both convective and chemical contributions. Reconstructed surface heating profiles generated by this approach were informative and valuable in comparing surface heating variations at different locations on the heatshield; however, an important limitation of this approach was the lack of a straightforward way

to compare reconstructed surface heating with CFD heating predictions. As a part of this study, a Monte Carlo analysis was also performed to quantify the uncertainty associated with the reconstructed heating profiles based on thermocouple measurement uncertainty and material property variations.

The current plan for reconstruction of MEDLI2 thermocouple data is to apply the same approach that was utilized for MEDLI data, with improved techniques and models. As mentioned before, the main limitation faced during MEDLI reconstruction was the lack of a validated finite-rate chemistry model for PICA in a Martian atmosphere. A finite-rate model, which is currently being developed by the NASA Entry System Modeling project, would greatly improve the value gained from in-depth thermocouple data. This would enable estimation of surface film coefficient and a more straightforward comparison of reconstructed heating profiles with CFD predictions. Another proposed improvement is a more detailed assessment of uncertainties associated with input parameters in reconstruction process, including characterization of variations in thermophysical properties of flight-lot PICA material and a more detailed assessment of thermocouple measurement and depth uncertainty.

The addition of the heat flux sensors on the vehicle's aftbody provides an opportunity to infer surface heating due to the proximity of the sensors to the thermal plug locations. The MEDLI2 project is investigating new reconstruction techniques to merge multiple data sources in heating reconstruction. These techniques are commonly used in trajectory reconstruction field and take into account the uncertainty associated with the data from each instrument in the reconstruction process.

VIII. Summary

MEDLI2 will support key goals and objectives to improve aerodynamics, aerothermodynamics, and TPS response predictions and design margins. The data collected from the instrumentation suite builds upon the data from MEDLI, and supplies key measurements that were not collected previously, including afterbody pressure, convective and radiative heating, and forebody supersonic pressure data. These data are critical for informing and improving future missions to Mars, including small and large robotic missions, as well as human-crewed mission concepts. The measurements will reduce design uncertainties for future planetary entry missions beyond Mars and allow for more optimized performance during EDL.

References

- [1] Cheatwood, F.M., Bose, D., Karlgaard, C.D., Kuhl, C.A., Santos, J.A., Wright, M.J., "Mars Science Laboratory (MSL) Entry, Descent, and Landing Instrumentation (MEDLI): Complete Flight Data Set," NASA TM-2014-218533 (2014).
- [2] Karlgaard, C.D., Kutty, P., Schoenenberger, M., Munk, M.M., Little, A., Kuhl, C.A., and Schidner, J., "Mars Science Laboratory Entry Atmospheric Data System Trajectory and Atmosphere Reconstruction," *J. Spacecraft and Rockets*, Vol. 51, No. 4, July-August 2014.
- [3] Bose, D., White, T., Mahzari, M., and Edquist, K., "Reconstruction of Aerothermal Environment and Heat Shield Response of Mars Science Laboratory," *J. Spacecraft and Rockets*, Vol. 51, No. 4, July-August 2014.
- [4] NASA Technology Roadmaps, "TA-9: Entry, Descent, and Landing Systems," URL: http://www.nasa.gov/sites/default/files/atoms/files/2015_nasa_technology_roadmaps_ta_9_entry_descent_landing_final.pdf, July 2015.
- [5] Karlgaard, C., Kutty, P., and Schoenenberger, M., "Coupled Inertial Navigation and Flush Air Data Sensing Algorithm for Atmosphere Estimation," AIAA Paper 2015-0526, January 2015.
- [6] Brandis, A., Cruden, B., White, T., Saunders, D., and Johnston, C., "Radiative Heating on the After-Body of Martian Entry Vehicles," *45th AIAA Thermophysics Conference, AIAA Aviation*, AIAA Paper 2015-3111, 2015.
- [7] Cruden, B., Brandis, A., White, T., Mahzari, M., Bose, D., "Radiative Heating for MSL Entry: Verification of Simulations from Ground Test to Flight Data," *53rd AIAA Aerospace Sciences Meeting*, AIAA Paper 2015-1894, Jan 2015, Kissimmee, Florida.
- [8] Ried, R. C., Jr., Rochelle, W. C., Milhoan, J. D., "Radiative heating to the Apollo command module: Engineering prediction and flight measurement," NASA TM-X-58091, 1972.
- [9] Karlgaard, C., Van Norman, J., Siemers, P., Schoenenberger, M., and Munk, M., "Mars Entry Atmospheric Data System Modeling, Calibration, and Error Analysis," NASA TM-2014-218535, October 2015.

- [10] Siemers, P., Bradley, P., Wolf, H., Flanagan, P., Weilmuenster, K., and Kern, F., "Shuttle Flight Pressure Instrumentation: Experience and Lessons Learned for the Future," *NASA Langley Conference on Shuttle Performance: Lessons Learned*, Hampton, VA, March 1983.
- [11] Gibson, L. and Sealey, B., "Test and Evaluation of Pressure Transducers for a Reentry Vehicle Pressure Measurement System," *39th International Instrumentation Symposium*, May 1993, pp. 1013-1030.
- [12] Karlgaard, C., Kutty, P., Schoenenberger, M., Munk, M., Little, A., Kuhl, C., and Shidner, J., "Mars Science Laboratory Entry Atmospheric Data System Trajectory and Atmosphere Reconstruction," *Journal of Spacecraft and Rockets*, Vol. 51, No. 4, 2014, pp. 1029-1047.
- [13] Mahzari, M., Braun, R., White, T., and Bose, D., "Inverse Estimation of the Mars Science Laboratory Entry Aeroheating and Heatshield Response," *Journal of Spacecraft and Rockets*, Vol. 52, No. 4, 2015, pp. 1203–1216.